

# Short Visit Grant 3627

## Scientific Report: Split ring gold nanoparticles as potential plasmonic biosensors

Philipp Schöffner

Institute of Physics, Karl-Franzens-University, 8010 Graz, Austria

### Purpose of the visit

Gold and silver nanoparticles support localized surface plasmons (LSPs) that can be excited optically, resulting in scattering and absorption resonances. These resonances strongly depend on the particle geometry (size and shape) and on the refractive index of the surrounding medium close to the surface of the particles. The latter dependence can be exploited to build nanoscale biosensors: Molecules adsorbed to the particle surface lead to a spectral shift of the LSP resonances. The quantity of this shift is related to the local optical field strength, with strong fields leading to strong shifts and thus high sensitivity in sensor applications.

In this project we focus on ring geometries featuring a slit (“split ring”) offering two main advantages. First, the variation of the geometry parameters of split rings allows the tuning of the LSP mode profile and field enhancement (specifically in the gap) in a rather broad range. Second, for a given geometry (and illumination condition) it is possible to switch the mode profile and enhancement by simple polarization control [1]. Our work program is dedicated to clarifying how these variations determine the spectral profiles of the split rings and their potential for sensing.

At our home institution, we are experienced in fabricating metal nanoparticles (including split rings) with lateral feature sizes reproducible to within less than 5 nm using electron beam lithography. The hosting institution offers the expertise in the chemical synthesis necessary to vary the local optical properties of the particle environment in a defined manner. Therefore, the combined expertise and infrastructure enabled us to tackle the points raised above.

The main purpose of the visit was to, first, spectrally characterize single lithographically fabricated gold split rings and, as a reference, ring-shaped nanoparticles. Second, these measurements should be extended to particles with different dielectric environ-

ments tuned by the bonding of DNA complexes via immobilized (capture) DNA on the particle surface.

## Work carried out and main results

Prior to the visit at the host institution, gold nanoparticles with three different shapes - disc, ring and split ring - were fabricated using electron beam lithography and thermal evaporation in combination with a liftoff process. As substrate, ITO doped glass was used, ensuring electric conductivity required for the electron beam exposure. Particles with the same shape and nominal size were arranged in an  $11 \times 11$  array with an equal particle separation of  $5 \mu\text{m}$ , suitable to measure single particle spectra. The lateral particle dimensions were measured with a SEM (see figure 1), whereas the structure height was determined via AFM measurements and found to be  $h = 32 \pm 2 \text{ nm}$ .

At the host institution, the nanoparticles were optically characterized by acquiring single particle scattering spectra. Therefore a ZEISS Axio Imager.Z1m microscope in combination with a fiber-optically connected monochromator of type SpectraPro 2300i of Princeton Instruments was used. In this setup, the glass substrate with the structures on top is illuminated from below using a dark field immersion condenser ( $\text{NA} = 1.2 - 1.4$ ), such that only light scattered from the particles on the top side is collected by a microscope objective ( $100\times$ ,  $\text{NA} = 0.9$ ). For spectral analysis, the structure plane is imaged on a fibre coupled to the spectrometer. The detection spot-size is approximately  $2 \mu\text{m}$  in diameter, allowing for real single particle measurements.

Figure 2 exemplarily shows the scattering spectra for the three different particle shapes. The resonance peak of the disc-like particle corresponds to the dipolar LSP mode and lies at around  $680 \text{ nm}$ , whereas that of the ring results from excitation of the symmetric dipole mode with the resonance at  $900 \text{ nm}$  [2]. The split ring, instead, shows two distinct peaks. To elucidate the character of the excited LSPs, numerical calculations based on a boundary element method were performed [3]. The insets in figure 2 depict the surface charge densities in arbitrary units calculated within the quasi-static approximation. The lower-order mode (LSP resonance at  $840 \text{ nm}$ , denoted as  $n=2$  mode, referring to the node number in the surface charge distribution) resembles the symmetric dipole mode of the ring, whereas the higher-order mode (LSP resonance at  $700 \text{ nm}$ , denoted as  $n=4$  mode, one node being in the gap) is unique for the split ring. For the latter, the high charge concentration at the ends of the split ring arms generates strong optical fields concentrated in a small volume around the gap [1]. This makes it a potential candidate for (bio-)sensing applications requiring high spatial resolution in the order of tens of nanometers. For the  $n=2$  mode, the field in the interior part of the split ring is almost homogeneously distributed.

In order to investigate the variation of the LSPRs due to changes in the refractive index in the immediate surrounding medium, in a first step, monolayers of thiolated single-stranded deoxyribonucleic acid (ssDNA) were bonded to the structures. In a second step, this immobilized DNA was hybridized with a complementary target DNA-strand serving as analyte. After every step, scattering spectra of the same particles

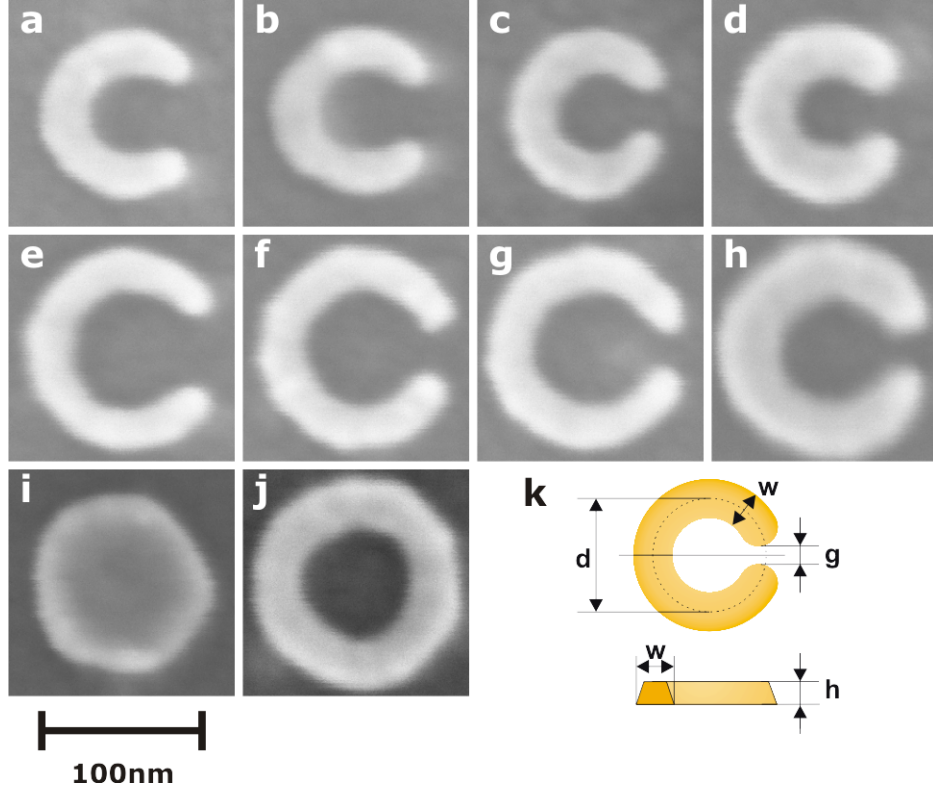


Figure 1: SEM images of selected gold nanoparticles fabricated on ITO doped glass substrates using electron beam lithography (EBL). (a)-(d) Split rings with a mean diameter of  $D = 78 \pm 3 \text{ nm}$ , a width of  $w = 29 \pm 2 \text{ nm}$  [(a)-(c)] and  $w = 34 \pm 2 \text{ nm}$  [(d)], respectively, and a gap size of  $g = \{40, 31, 25, 25\} \pm 4 \text{ nm}$ . (e)-(h) Split rings with  $D = 100 \pm 3 \text{ nm}$ ,  $w = 26 \pm 2 \text{ nm}$  [(e)-(g)] and  $w = 36 \pm 2 \text{ nm}$  [(h)], respectively, and gap size  $g = \{44, 25, 21, 18\} \pm 4 \text{ nm}$ . (i) Disc with diameter  $D = 110 \pm 5 \text{ nm}$ . (j) Ring with mean diameter  $D = 98 \pm 3 \text{ nm}$  and width  $w = 32 \pm 2 \text{ nm}$ . The errors are standard deviations of geometry parameters of particles within the same arrays. For all structures the height is  $h = 32 \pm 2 \text{ nm}$ . (k) Definition of the geometry parameters and schematic of the cross section profile for EBL particles.

were acquired. In detail, for the first step, the immobilization of the capture DNA, the samples were plasma etched and subsequently incubated in an aqueous solution of  $1 \mu\text{M}$  of thiolated ssDNA containing 30 base pairs in 1 M potassium phosphate serving as buffer, for 120 minutes with constant shaking. Then the samples were rinsed in water and dried with  $\text{N}_2$  gas. The hybridization of the target ssDNA was accomplished in almost the same manner, but with  $1 \mu\text{M}$  ssDNA containing 20 complementary base pairs and 2x-SSC (saline-sodium citrate buffer) as hybridization buffer instead.

Figure 3 shows the relative resonance shifts of the split rings (figure 1) for both LSP

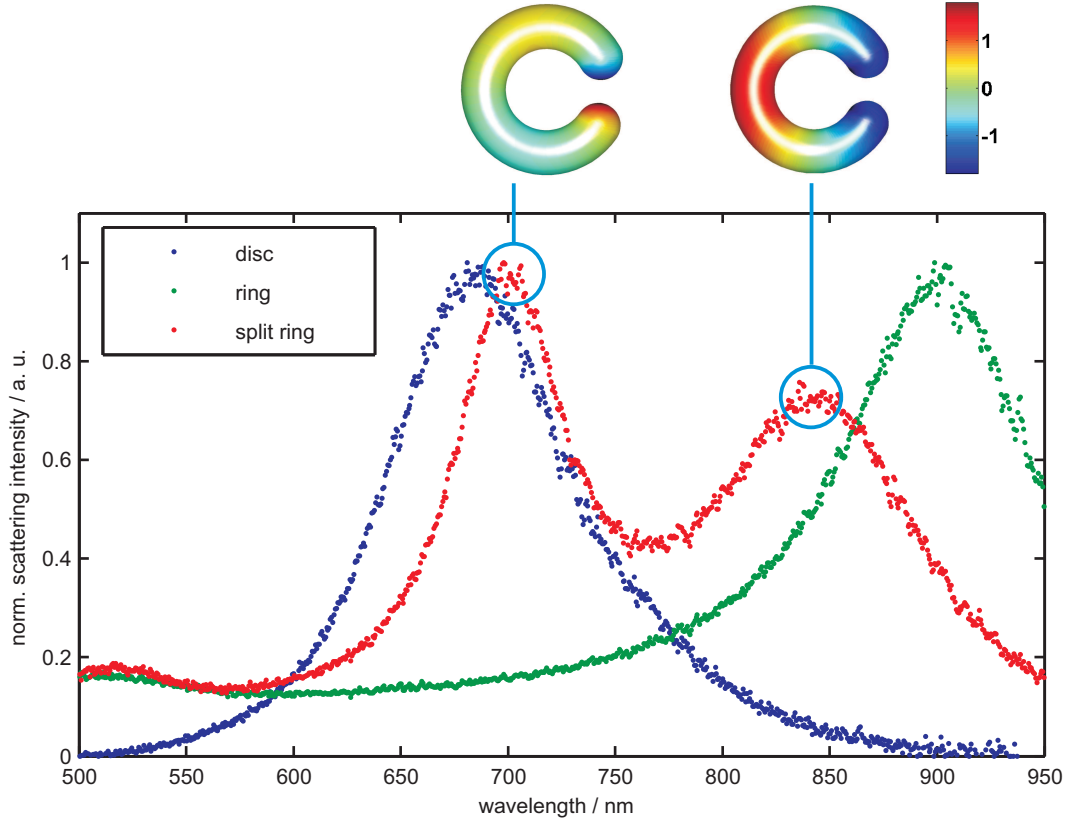


Figure 2: Single particle scattering spectra for a disc, a ring and a split ring with geometry parameters according to figure 1 (i), (j) and (h), respectively. The insets show the surface charge densities (in arbitrary units) for the excited LSP of the split ring, which were numerically calculated based on a boundary element method.

modes versus the particle gap size  $g$  and sorted by the mean diameter  $D$ , upon bonding of the analyte (target ssDNA) to the particle surface. The absolute spectral shift ( $\Delta\lambda_n$ ) was found to be up to  $5 \pm 2$  nm for the  $n=4$  mode and up to  $7 \pm 1$  nm for the  $n=2$  mode. Expressed in relative shifts  $\Delta\lambda_n/\lambda_{n,im}$ , with  $\lambda_{n,im}$  being the resonance wavelength of the mode  $n$  with immobilized ssDNA bonded to the particle, this gives  $0.7 \pm 0.3$  % and  $0.9 \pm 0.2$  %, respectively (figure 3). We assumed that, especially for the higher-order  $n=4$  mode, the amount of shift increases as the gap size reduces, because of a higher field enhancement in the gap area. However, as is obvious from figure 3, the variation within our data is very high, so that no direct correlation with the gap size (nor with other particle geometry parameters) can be seen. This strong variation might be due to a nonuniform bonding behaviour of the thiolated ssDNA to the single particles. And as for the gap size dependence, the reduction of detection volume with decreasing gap size may counteract the effect of optical field enhancement.

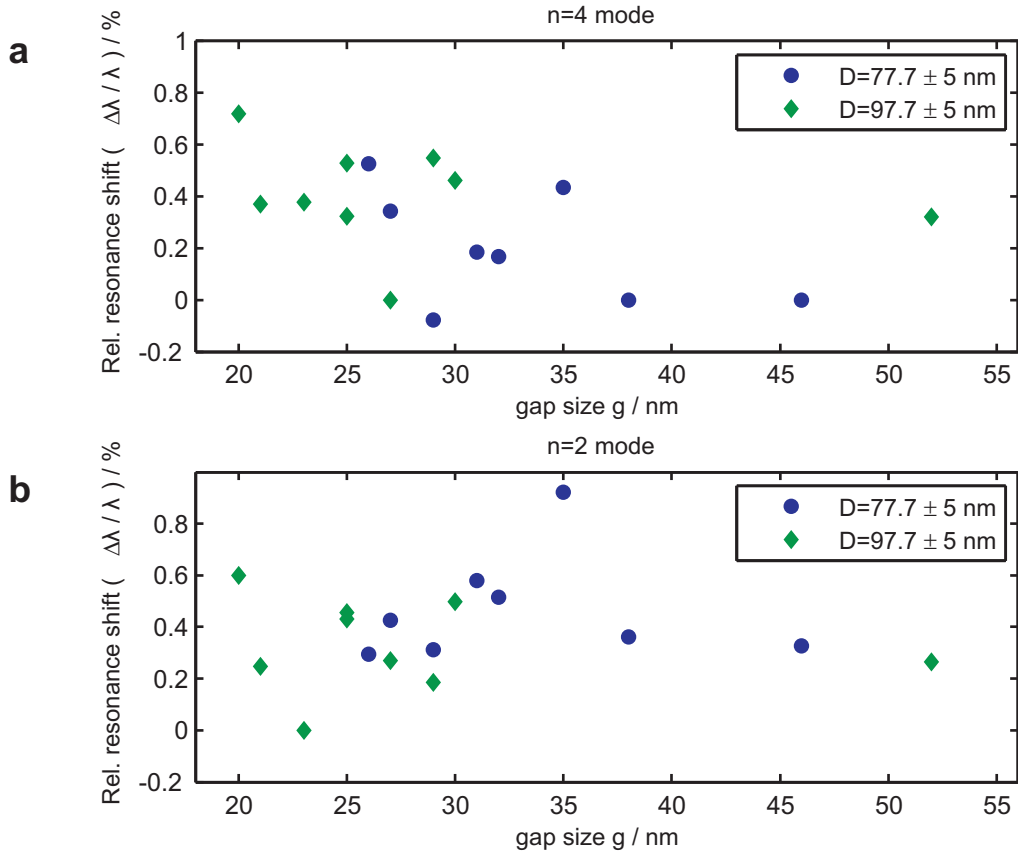


Figure 3: Relative shift of LSP resonances of split ring particles for (a) the higher order  $n=4$  mode and (b) the lower order  $n=2$  mode upon bonding of the target ssDNA to the immobilized capture DNA. The blue dots and green dots, respectively, represent the mean values for split rings with mean diameters within  $D = 77.5 \pm 5$  nm and  $D = 97.5 \pm 5$  nm. The spectral positions of the LSP resonance peaks were determined after box car averaging the spectral data.

For comparison, it was intended to additionally measure the sensitivity of the disc- and ring-type structures, but unfortunately the optically characterized particles were washed off the substrate during the second, hybridization step. However, Larsson, E. M., et al. investigated the LSPR shift of ensembles of nanorings prepared by means of colloidal lithography upon bonding monolayers of proteins such as biotinylated bovine serum albumin and subsequently neutravidin on the particle surface [4]. The reported resonance shift, expressed as relative shift, is  $0.40 \pm 0.13$  % for biotin-BSA bonding and  $0.30 \pm 0.03$  % for subsequent bonding of neutravidin. Although a direct comparison is not possible due to the different measuring condition and bonding behaviour, this shift is of the same order as we observed here with the split rings, which have a presumably

much smaller sensing volume.

## Future collaboration and projected publications

Future collaborations with the hosting institution are planned to further investigate the relationship between optical field enhancement in the gap and sensitivity to the bonding of analytes via the method discussed herein. This also includes the question for the lower limit of detection volume for biomolecules exploiting the higher order  $n=4$  mode of split rings.

A publication in a field related journal such as NANO LETTERS is projected. Therefore the problem of strong variation in the resonance shift has to be addressed. Also the comparison of the sensitivity for split ring, disc and ring nanoparticles under the same experimental conditions has to be carried out beforehand.

## References

- [1] A. W. Clark, A. Glidle, D. R. S. Cumming, and J. M. Cooper. Plasmonic Split-Ring Resonators as Dichroic Nanophotonic DNA Biosensors. *JOURNAL OF THE AMERICAN CHEMICAL SOCIETY*, 131(48):17615–17619, DEC 9 2009.
- [2] J. Aizpurua, P. Hanarp, D. S. Sutherland, M. Kall, G. W. Bryant, and F. J. G. de Abajo. Optical properties of gold nanorings. *PHYSICAL REVIEW LETTERS*, 90(5), FEB 7 2003.
- [3] U. Hohenester and J. Krenn. Surface plasmon resonances of single and coupled metallic nanoparticles: A boundary integral method approach. *PHYSICAL REVIEW B*, 72(19), NOV 2005.
- [4] E. M Larsson, J. Alegret, M. Kall, and D. S. Sutherland. Sensing Characteristics of NIR Localized Surface Plasmon Resonances in Gold Nanorings for Application as Ultrasensitive Biosensors. *NANO LETTERS*, 7(5):1256–1263, MAR 2007.